Validation of Transient Module in RAST-F Code for Fast Reactor Analysis

Tuan Quoc Tran, Deokjung Lee*
Department of Nuclear Engineering, Ulsan National Institute of Science and Technology
50 UNIST-gil, Ulsan, 44919, Republic of Korea
trantuan@unist.ac.kr, deokjung@unist.ac.kr

1. Introduction

The RAST-F code system has been under development for fast reactor core analysis purposes. In order to provide a reliable tool for core behavior predictions, the validation and verification of state-of-the-art computational tools and associated databases are the first key step. There were several verification and validation work for RAST-F, while most of them focused on the k-eigenvalue and depletion calculations [1-3]. In the framework of the RAST-F developments, a neutron transient module has been implemented in RAST-F at the core level, which enables to simulate the prompt and delayed neutron emission model. For further development, theoretical calculations and computer modeling of this new implementation need experimental validation.

Among the benchmark sets for validating, verifying, and improving methodologies and computer codes, the CEFR benchmark [4] has unique design features such as using very highly enriched fuel, a small core-size reactor, and stainless-steel reflectors. These characteristics may result challenging in predicting accurately the neutronic parameters for the simulation tools, especially the deterministic code system.

In this study, the time-dependent simulation of the CEFR control rod drop experiment was performed using nodal diffusion code RAST-F. The comparison between simulation and measurement was conducted on relative neutron population, dynamic reactivity, and control rod worth. The main goal of this paper is to demonstrate and validate the transient modeling capability of the RAST-F code by comparing the RAST-F results to the experimental data.

2. Description of CEFR and CR drop experiments

The CEFR is a pool-type sodium-cooled fast reactor in China with thermal power of 65 MW and electric power of 20 MW. CEFR reached its first criticality in July 2010. In the physical start-up tests in 2010, four series of experiments were conducted, including fuel loading and criticality, measurement of the control rod worth, measurement of reactivity coefficient, and foil activation measurements. The physical start-up experiments have three different stages of the core: the fuel-only loading, the operating loading at the cold state, and the operating loading at the hot state. In this study, all physical start-up tests were conducted at cold state (250 °C). The core at operating loading consists of 79 fuel sub-assemblies, as illustrated in Fig. 1. The active fuel height of the core is 45 cm. FA pitch is 6.1 cm. In addition, the core was loaded with 8 control, and 1 neutron source, 394 Stainless steel reflectors, and 230 boron shield sub-assemblies. The core reactivity is controlled by three types of control rod sub-assemblies: two regulating rods (RE), three shim rods (SH), and three safety rods (SA). The main difference between the three types of control rod sub-assemblies is the enrichment of ^{10}B in the B$_4$C absorber. The enrichment of ^{10}B in regulating, shim, and safety rods are 19.6 a% (natural abundance), 92 a%, and 92 a%, respectively. Corresponding to the mass of ^{10}B in each control rod, the RE rods are used for maintaining the small reactivity, while the SH and SA rods are used for the compensation of large reactivity change and emergent shut-down, respectively. A detailed description of the geometry, materials, and experiments can be found in Refs. [4-6].
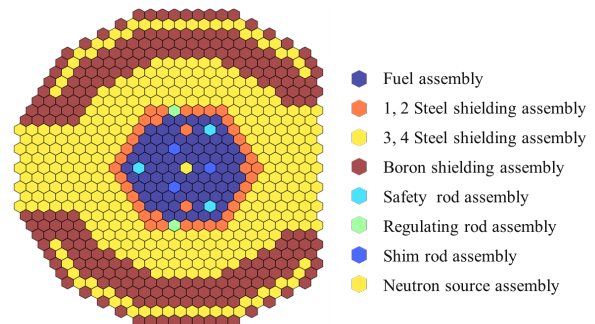
Fig. 1. Core configuration at operating load.

According to the specification of the benchmark, the control rod worth (CRW) measurements were carried out in two movement procedures, rod-drop, and normal speed movements. The measurement by the normal movement was excluded from the benchmark due to the extremely time-consuming process for neutronic simulation. On the other hand, the measurement by the rod-drop is much more painless. In the beginning, the measured rod was withdrawn to the out-of-core position, and other rods were altered properly to maintain a slightly supercritical system. After adjusting the control rod positions, the neutron flux increase. Two source range detectors were used and connected to a reactivity meter to measure the counting rate and calculate the reactivity in real-time. When the count rate from the detector reached a certain count per second, the measurement of the CRW started, and the measured rod was dropped. By that time, the reactivity meter recorded the count rate every 0.1s and calculated the reactivity based on the inverse kinetics method. No

spatial correction or dynamic corrections were conducted. All kinetics parameters were calculated by deterministic code for all calculations throughout the start-up experiments. The delayed neutrons are divided into 6 groups based on the life of the precursor. The decay constants of each group are calculated by the average of all fission nuclides [4].

3. Simulation

3.1. XS generation

All XSs were generated using the MCS code [7] for the application in RAST-F core calculation. The XS was generated on the 24-group energy structure. All calculations were performed using ENDF/B-VII.1 nuclear data files at 250 °C. The thermal expansion effect was considered in this simulation. The MCS simulations were performed for XS generation using 20 inactive cycles, 100 active cycles, and 100,000 neutron histories per cycle for fuel and non-fuel regions. Furthermore, the standard deviation in the flux magnitude was less than 1.2% for the thermal energy region. The SPH factors were applied for control and adjacent fuel sub-assemblies when the control sub-assembly was inserted into the active core region.

a) Non-fuel model   b) CR model

c) Blanket model   d) Enriched fuel model

e) Enriched fuel model
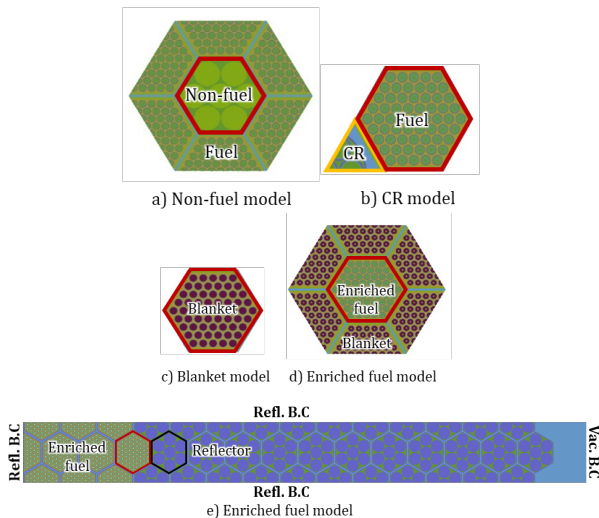
Fig. 2. The models for XS generations.

The XS for the non-fuel region was generated using a 2D supercell model (as in Figure 2a). The non-fuel hexagonal region is located in the center and surrounded by six highly enriched fuel (HEU) sub-assemblies. The boundary condition was reflective in the axial and radial directions. The XS for the absorber region in the control sub-assembly and nearby fuel region was prepared using a 2D supercell model (as in Figure 2b). The super-homogenization method was applied to correct the XSs in the case of the control sub-assembly shift. The XS for the blanket (LEU) region was generated using a 2D single model (as in Figure 2a). The XS for the HEU region was generated using a

2D supercell model (as in Figure 2d). The non-fuel hexagonal region is located in the center and surrounded by six HEU sub-assemblies. The boundary condition was reflective in the axial and radial directions. The 2D fuel-reflector model was used to generate XS for the most outer fuel region and nearby radial reflector region with an axial reflective boundary condition, as illustrated in Figure 2e.

3.2. RAST-F simulation

In the 3D core simulation, RAST-F performed calculations with 47 axial meshes and with radial and axial black boundary conditions. The thermal expansion was considered in both axial and radial directions. The rod-drop simulation was carried out using the XS generated by MCS, delayed neutron spectrum from SERPENT code [8], and point kinetic data provided by CIAE. In all simulated cases, the rod drop process was initiated at t = 0.5 sec, and the total simulated time interval was seven seconds for all cases. After the insertion, the CR remained in the core, and no other changes in the model geometry or composition were made.

4. Numerical results

In this study, the calculation is limited to the measurements of the CRW of individual safety CRs and the second shutdown group (three control sub-assemblies). The time-dependent normalized neutron population, dynamic reactivity, and CRW results from RAST-F are compared against the measured results in this section. It should be noted that the measured values of normalized neutron population and reactivity were obtained by the measured neutron count rates from two source range detectors (detector #1 and detector #2). In contrast, the normalized neutron population and reactivity of RAST-F are the core average values from the 3D core transient module. The temporal evolution of the neutron population is compared in Fig. 3. The comparison of the dynamic reactivity is plotted in Fig. 4. In general, the RAST-F computational results are in excellent agreement with measured results for normalized neutron population and reactivity in the simulation time. The dynamic CRW was obtained by a linear fitting in reactivity after the CR was fully insertion in the active core, from 0.95 s to 5 s for the individual rods and from 0.95 s to 7 s for the second shutdown group. The calculated CRWs include the results obtained with the static and time-dependent methods that are compared against the measured CRWs. The numerical values are presented in Table I. The "Meas.", "Static", "Dyn.", and "Diff." abbreviations in Table I stand for measurement, static, time-dependent solutions, and the difference between measurements and calculated values. The results presented in Table I demonstrate a very good agreement between the experiment and simulations as well as

among the applied computational approaches. All calculated CRWs agree well within less than one standard deviation with the corresponding measured values. The discrepancy between the calculated and measured CRWs is less than 60 pcm for the individual CRs simulations and less than 200 pcm for the second shutdown group.
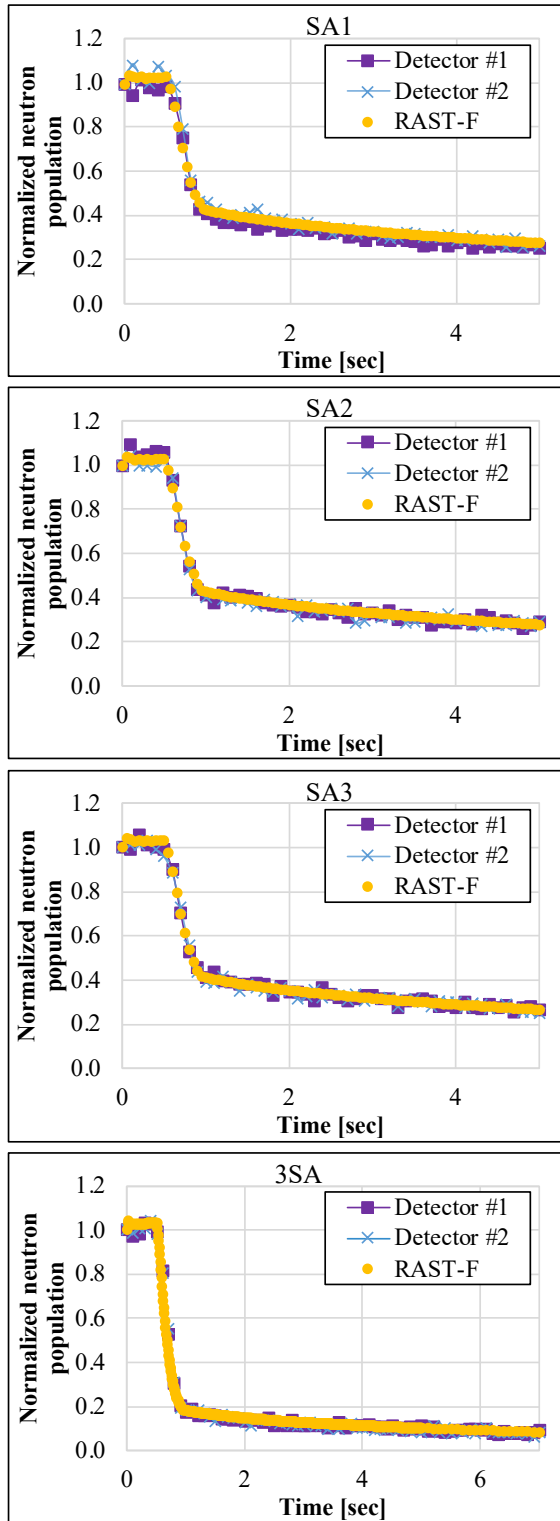
Fig. 3. Normalized neutron population comparison.
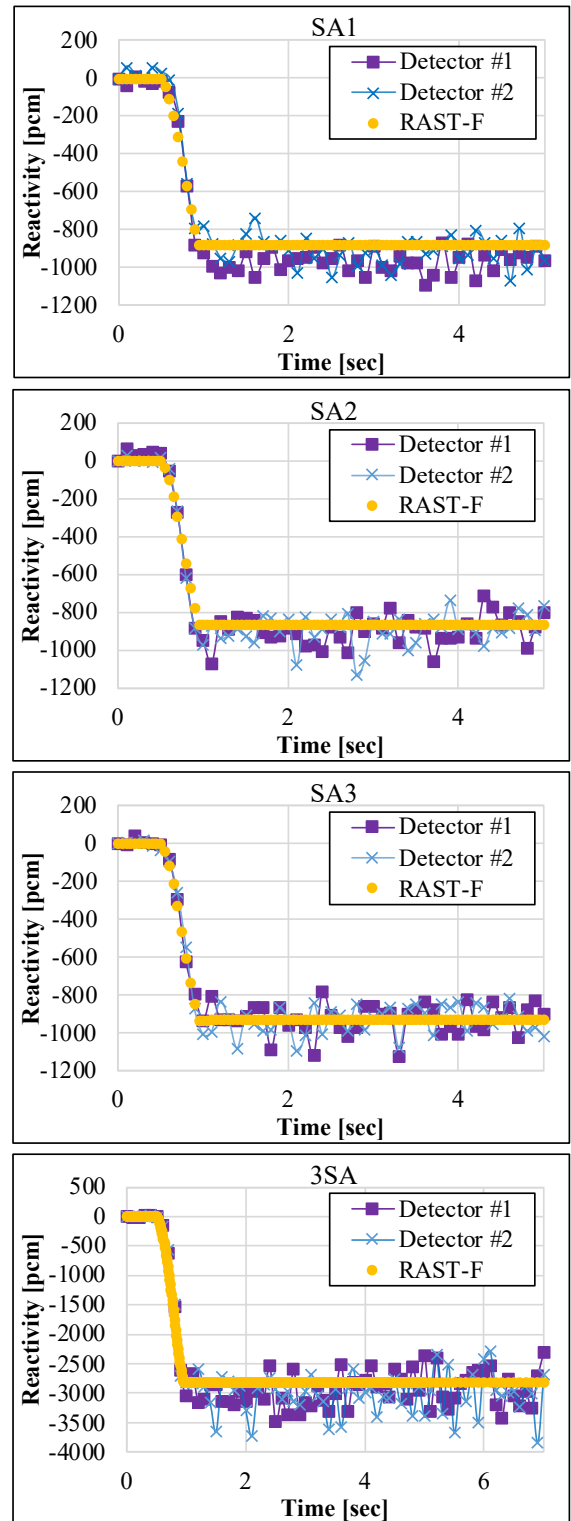
Fig. 4. Dynamic reactivity comparison.

Table I. CRW comparison.

CRs	CRW (pcm)			Diff. (pcm)	
	Meas.	Static	Dyn.	Static	Dyn.
SA1	945 ± 100	916	885	−29	−60
SA2	911 ± 100	958	866	47	−45
SA3	946 ± 98	932	932	−14	−14
3SA	2981 ± 395	2957	2810	−24	−171

5. Conclusion

In this study, the CEFR CR drop experiment was simulated to validate the transient capability of the nodal diffusion code system RAST-F to strengthen the accuracy of diffusion solutions. The homogenized XS generation by MCS Monte-Carlo code was used in RAST-F code for the 3D core simulation. The calculation results, such as normalized neutron population, dynamic reactivity, and CRWs, were compared to the experimental data. In comparing neutron population and reactivity, the RAST-F results are almost identical with the measurement for all cases. The calculated CRWs in both static and time-dependent methods show a good agreement with measurement data within one sigma.

Overall, the transient capability was successfully tested against the CEFR experiments indicating that the RAST-F code system can be used for the FR transient analysis. In addition, this work contributes to validating the RAST-F code system for neutronic core analysis. In the future, the investigation on other benchmarks will be conducted to strengthen the time-dependent analysis capability of RAST- F for FR.

ACKNOWLEDGMENTS

REFERENCES

[1] T.Q. Tran, et al., "Verification of A Two-Step Code System MCS/RAST-F to Fast Reactor Core Analysis," Nucl. Eng. Tech., https://doi.org/10.1016/j.net.2021.10.038 (2021).
[2] T.Q. Tran, et al., "Verification of a depletion solver in RAST-K for Fast Reactor Analysis," KNS Winter Meeting, Korea (online), Dec 16-18 (2020).
[3] T.Q. Tran, D. Lee, "Neutronic Simulation of the CEFR Experiments with the Nodal Diffusion Code System RAST-F," Nucl. Eng. Tech., 54(7), pp. 2635- 2649, https://doi.org/10.1016/j.net.2022.01.027 (2022).
[4] X. Huo, et al., "Technical Specifications for Neutronics Benchmark of CEFR Start-Up Tests," IAEA CRP-I31032, CIAE, Beijing (2019).
[5] T.Q. Tran, et al., "Neutronic simulation of China experimental fast reactor start-up test- Part II: MCS Monte Carlo code calculation," Ann. Nucl. Energy, 148, https://doi.org/10.1016/j.net.2022.01.027 (2020).
[6] E. Fridman, X. Huo, "Dynamic simulation of the CEFR control rod drop experiments with the Monte Carlo code Serpent," Ann. Nucl. Energy, 148, https://doi.org/10.1016/j.anucene.2020.107707 (2020).
[7] T.D.C. Nguyen, H. Lee, D. Lee, "Use of Monte Carlo Code MCS for Multigroup Cross Section Generation for Fast Reactor Analysis", Nucl. Eng. Tech., 53(9): 2788-2802, (2021).
[8] J. Leppänen, M. Pusa, T. Viitanen, V. Valtavirta, T. Kaltiaisenaho, "The Serpent Monte Carlo code: Status, development and applications in 2013", Ann. Nucl. Energy, 82 (2015), pp. 142-150.